

# Azido-Functionalized Thiophene as a Versatile Building Block To Cross-Link Low-Bandgap Polymers

Christian J. Mueller,<sup>†</sup> Tobias Klein,<sup>†</sup> Eliot Gann,<sup>‡,§</sup> Christopher R. McNeill,<sup>§</sup> and Mukundan Thelakkat<sup>\*,†</sup>

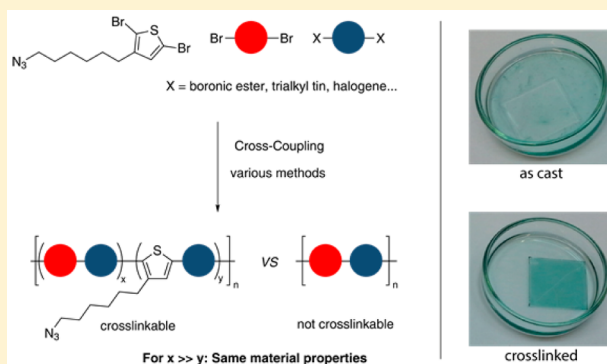
<sup>†</sup>Applied Functional Polymers, Macromolecular Chemistry I, University of Bayreuth, 95440 Bayreuth, Germany

<sup>‡</sup>Australian Synchrotron, 800 Blackburn Road, Clayton, VIC 3168, Australia

<sup>§</sup>Department of Materials Science and Engineering, Monash University, Wellington Road, Clayton, Victoria 3800, Australia

## Supporting Information

**ABSTRACT:** We unveil a concept for the design of cross-linkable semiconducting polymers that is based on a modular tercopolymerization which stands out by its low synthetic effort, easy accessibility, and its broad range of applications. 3-(6-Azidohexyl)thiophene was used as a comonomer in the synthesis of a variety of low-bandgap copolymers using different polymerization techniques such as Suzuki–Miyaura cross-coupling and Stille cross-coupling. We show that when only a small amount (5–10 mol %) of azide groups is introduced into the polymers, the impact on absorption and electrochemical properties (HOMO/LUMO values) is negligible. The small amount of azide functionality is however enough to obtain polymers that can easily be cross-linked by UV illumination. Thermal stability of the solid state packing and alignment is studied in neat polymer thin films as well as in blends with [6,6]-phenyl-C<sub>71</sub>-butyric acid methyl ester (PC<sub>70</sub>BM) as a relevant model blend system. Solvent resistivity of these polymer films is investigated by absorption and photoluminescence measurements. It is finally shown in organic field effect transistors that the introduction of 10% azide-functionalized monomer does not considerably influence hole transport mobility (0.20–0.45 cm<sup>2</sup> V<sup>-1</sup> s<sup>-1</sup>).



## INTRODUCTION

Since the successful introduction of polymer bulk heterojunction solar cells in 1995,<sup>1,2</sup> tremendous progress has led to bulk heterojunction solar cell devices exceeding 10% power conversion efficiency (PCE).<sup>3</sup> Aggregation and morphology control in the active layer of those bulk-heterojunction solar cells has been identified as an important key in accessing high-efficiency solar cells above 10% PCE.<sup>3</sup> When moving from the research level to commercial production, morphological stability becomes indispensable not only for long lifetimes but also for the particular processing methods. Roll-to-roll (R2R) printing with high throughput at appreciable web speeds, for example, demands fast drying of printed active layers, and the morphology must therefore be stable under repeated curing conditions which are commonly above 100 °C.<sup>4</sup>

Cross-linking of the polymer offers a viable route to stable morphologies as it allows for locking-in of the morphology<sup>5</sup> once an optimal condition has been attained, e.g., by tuning the printing parameters or postprocessing, such as thermal or vapor annealing.<sup>6</sup> Two different concepts have been shown to offer good cross-linking efficiency leading to thermally stable blends that exhibit very good PCE retention after aging the solar cells. In the first approach semiconducting polymers can be made cross-linkable by synthetically introducing cross-linkable groups

into the side chains of their respective monomers. These groups include alkyl halides, azides, oxetanes, or vinylenes that can then be used for cross-linking, mostly by UV curing.<sup>7–14</sup> In the case of cross-linking using azides, highly reactive nitrenes are formed which can undergo a variety of cross-linking reactions, such as C–H insertions, C=C cycloadditions, and other triplet reactions.<sup>12,14</sup> Taking into consideration that the new generation of donor–acceptor alternating copolymers are prepared from specifically functionalized monomers (e.g., borolanes, stannyl derivatives), this approach requires the laborious modification of one of the comonomers used; i.e., several additional synthetic steps are necessary to render a particular polymer system cross-linkable. This increases the material costs and thus impairs commercialization. The second concept relies on cross-linking using low molecular weight additives such as bisazides or dithiols.<sup>15–18</sup> In this approach, nonvolatile additives are introduced that might affect photo-physics of charge generation as well as charge transport and extraction in the final blends. Even though each cross-linkable functional group has its advantages and disadvantages, we concentrate in our work on azides to test the generality of our

**Received:** December 31, 2015

**Revised:** April 21, 2016

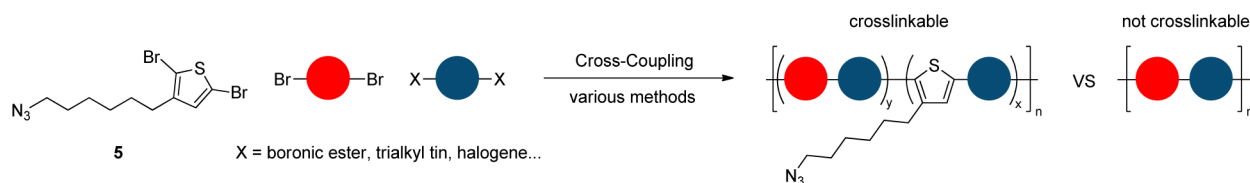


**Figure 1.** Modular concept for cross-linkable tercopolymers using 3-(6-azidoheptyl)thiophene as a building block for Stille or Suzuki polycondensation.

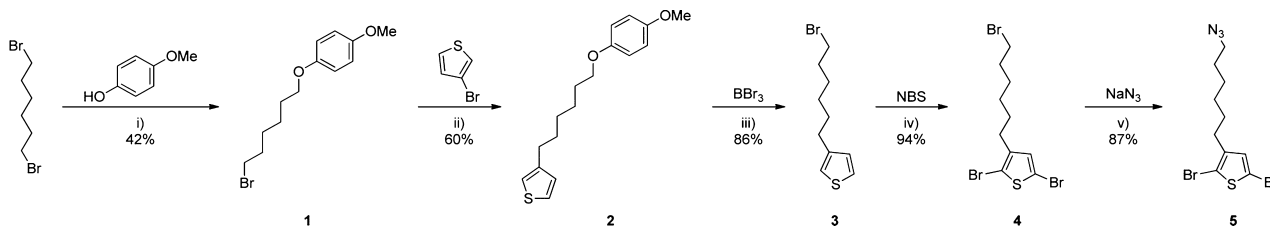


**Figure 2.** Synthesis of the azide-functionalized building block **5**. Reagents and conditions: (i) NaOMe, EtOH, 2 h, reflux; (ii) Mg, Et<sub>2</sub>O, Ni(dppp)Cl<sub>2</sub>, 3 days, reflux; (iii) DCM, 1.5 h, reflux; (iv) THF, 24 h, rt; (v) DMSO, 2 h, rt.

novel approach for different polymerization reactions. Azides are reported to cross-link via UV illumination due to the formation of nitrenes, which can then undergo alkyl side-chain insertion reactions.<sup>15</sup>

In this contribution, we unveil a third concept for cross-linking semiconducting polymers that is based on a modular tercopolymerization. We avoid the weaknesses of both above-mentioned concepts, namely, the synthetic effort of modifying monomers required for each particular polymer system and the dilution of electroactive materials and introduction of an at best electronically nonactive cross-linking additive. Instead, we show that a simple azide-functionalized thiophene comonomer can be used in small quantities in diverse polymerizations to give various tercopolymers with an azide content that allows efficient cross-linking but without altering any of the optical and electronical properties of the final polymers. This paves the way for effectively synthesizing various low-bandgap copolymers with inherent cross-linkability without the need of any additional synthetic steps to modify the respective electron-rich or electron-deficient monomers. A detailed analysis of structure formation and charge carrier transport is undertaken to evaluate the influence of cross-linking.

## RESULTS AND DISCUSSION

**Synthesis.** The synthetic strategy pursued in our cross-linkable tercopolymer approach is based on a versatile and common building block that can be applied to different semiconducting low-bandgap polymers without having too much influence on their final properties. We hence chose thiophene as an almost ubiquitous motif in conjugated polymers. The functional groups for polymerization were chosen to be bromines, not only in order to keep the synthesis route as short as possible but also mostly as it can be employed in many different polymerization techniques that are commonly used to synthesize state-of-the-art low-bandgap polymers, such as Stille, Suzuki, Yamamoto, Negishi, Kumada, and Heck cross-coupling polymerizations. It has also been shown earlier that no strictly alternating donor–acceptor sequence is required for lowering the optical gap and random or statistical copolymerization is a viable option.<sup>19,20</sup> When the azide-functionalized comonomer **5** is added in small quantities (less than 5 wt %) to AA/BB-type polycondensations, a cross-linkable tercopolymer

can be obtained that exhibits repeating units *y* which are identical to the regular strictly alternating copolymer and a repeating unit *x* consisting of the azido-functionalized thiophene **5** and the comonomer carrying the complementary functional groups.

The synthetic route of the azide-functionalized comonomer is shown in Figure 2. Starting from 1,6-dibromohexane, we followed a previously reported route<sup>21</sup> to obtain 3-(*p*-methoxyphenoxy)hexyl bromide **1**. Conversion into the Grignard compound and Kumada cross-coupling using 3-bromothiophene yielded 3-(6-(4-methoxyphenoxy)hexyl)thiophene **2**. The *p*-methoxyphenyl (PMP) protecting group was then cleaved off by the use of boron tribromide and the resulting intermediate simultaneously converted to the  $\omega$ -alkyl halide **3**.<sup>22</sup> Dibromination using *N*-bromosuccinimide almost quantitatively gave 2,5-dibromo-3-(6-bromohexyl)thiophene **4**, and finally a Finkelstein reaction using sodium azide yielded 3-(6-azidoheptyl)-2,5-dibromothiophene **5** which was used as the comonomer in tercopolymerizations. We preferred this route over a previously published one<sup>23</sup> in order to avoid a mixture of 2-(6-bromohexyl)thiophene and 3-(6-bromohexylthiophene) due to the “halogen shuffling” reaction after lithiation. This mixture is extremely hard to purify. The route shown here results in the desired substitution product via Grignard metathesis.

We chose four different polymer systems which were selected due to their promising semiconductor properties and widespread use in the literature: three from the diketopyrrolopyrrole (PDPP) family and one from the carbazole–benzothiadiazole (PCDTBT) family. PDPP[T]<sub>2</sub>-T (**P1–P4**) is a widely used and investigated low-bandgap donor for use in organic solar cells, also showing excellent field effect transistor mobilities.<sup>24–26</sup> PDPP[Py]<sub>2</sub>-T (**P5/P6**) was selected due to its remarkable *n*-type properties and promising bulk electron mobility.<sup>27</sup> PDPP[T]<sub>2</sub>-Ph (**P7/P8**) is another easily accessible and well-established donor polymer<sup>28</sup> used in solar cells which has gained a lot of interest due to the high power conversion efficiencies (7.4%) obtained with this material.<sup>29</sup> Finally, we also investigate a PCDTBT system (**P9/P10**) as another widespread donor material which is not based on diketopyrrolopyrroles.<sup>30</sup> Moreover, we verify the suitability of our approach for Suzuki as well as Stille polycondensations.

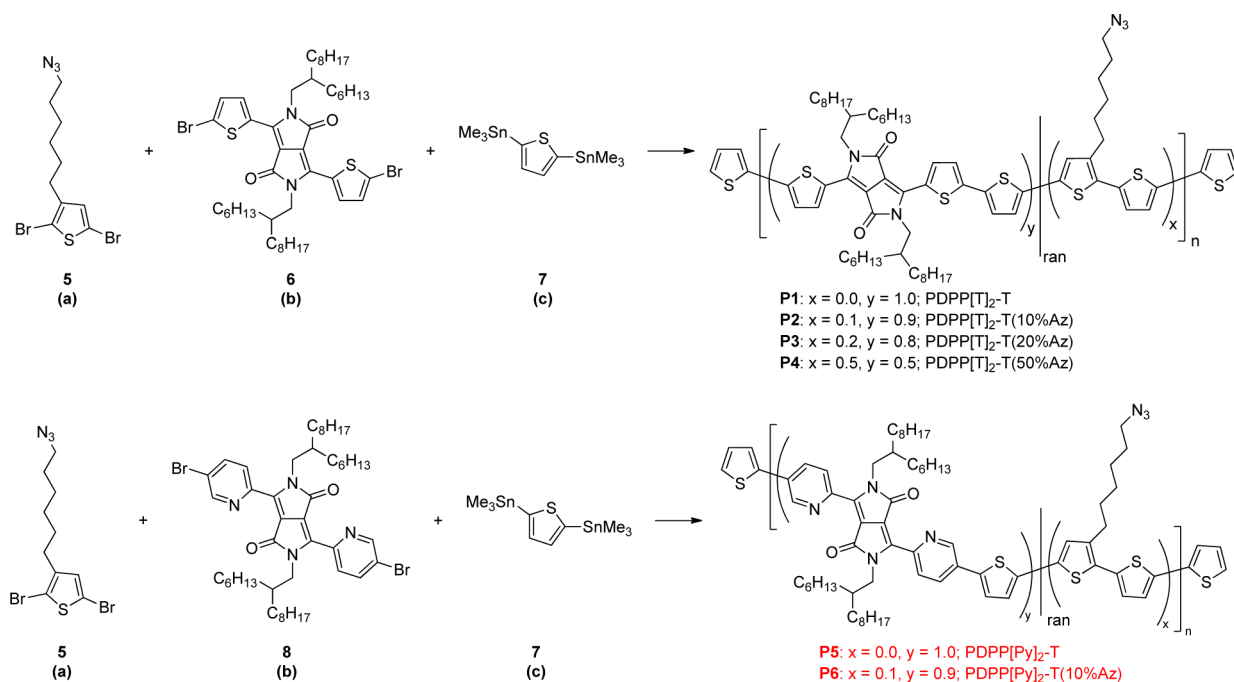


**Figure 3.** Stille polycondensations of typical hole conducting low-bandgap polymers PDPP[T]<sub>2</sub>-T (**P1–P4**) and typical electron conducting low-bandgap polymers PDPP[Py]<sub>2</sub>-T (**P5, P6**) with a varying degree of azide functionalization.

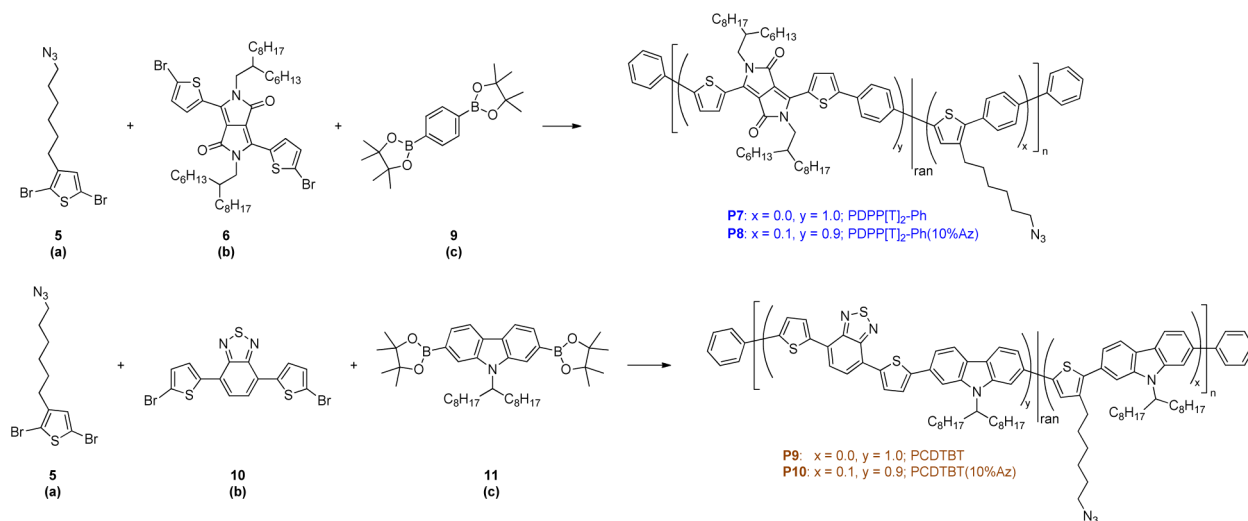


**Figure 4.** Suzuki polycondensation of a PDPP system PDPP[T]<sub>2</sub>-Ph (**P7, P8**) and another low-bandgap reference system PCDTBT (**P9, P10**) with and without azide functionalization.

For the cross-linkable PDPPs, polymerizations were performed by using either Stille polycondensation (see Figure 3) or Suzuki polycondensation (see Figure 4), whereas the cross-linkable PCDTBT was obtained via Suzuki polycondensation (Figure 4). All polymers were purified by repeated reprecipitations and Soxhlet extractions. The removal of unreacted monomers was verified using thin layer chromatography (TLC). Feed ratios ( $f_a, f_b, f_c$ ) of the three monomers **a**, **b**, and **c** as well as resulting built-in ratios determined by <sup>1</sup>H NMR spectroscopy are summarized in Table 1. The mole fractions  $\chi$  of the repeating units  $x$  and  $y$  determined by NMR are very similar to the calculated values expected from the feed ratio and are well within the error of polymer NMR spectroscopy. Detailed information on the calculation of the built-in ratio of the azido-functionalized thiophene comonomer is given in the

Supporting Information (section 5.1). It also is evident from the <sup>1</sup>H NMR that the azide group is suitable for the different polymerization conditions and survives in high yield under different reaction conditions by comparing the methylene protons next to the azide group ( $H_g$ ) and next to the thiophene core ( $H_b$ ). As given in Table S1 (see Supporting Information), the ratio is approximately 1 within the errors of polymer NMR spectroscopy. The molecular weights and the degrees of polymerization (DP) obtained from gel permeation chromatography (GPC) as well as the expected average number of azide moieties per polymer chain calculated from the feed ratio are summarized in Table 1. The elugrams of the individual polymers are shown in the Supporting Information. The azide-functionalized tercopolymers show similar molecular weights and degrees of polymerization compared to their non-

**Table 1. Molecular Characteristics of the Synthesized Polymers**

polymer	$f_a^a$	$f_b^a$	$\chi_f(y)$ [ $\chi_{\text{NMR}}(y)$ ] <sup>b</sup>	$\chi_f(x)$ [ $\chi_{\text{NMR}}(x)$ ] <sup>b</sup>	$M_n^c$ [kg/mol]	$M_w^d$ [kg/mol]	$D^e$	$DP^f$	$n(\text{N}_3)^g$	wt % (N <sub>3</sub> ) <sup>h</sup> [%]
PDPP[T] <sub>2</sub> -T system										
<b>P1</b>	0.00	0.50	1.00 [1.00]	0.00 [0.00]	36.9	146	3.94	44	0	0.0
<b>P2</b>	0.05	0.45	0.90 [0.92]	0.10 [0.08]	31.6	254	8.03	41	4	2.7
<b>P3</b>	0.10	0.40	0.80 [0.85]	0.20 [0.15]	22.2	84.6	3.82	31	6	5.7
<b>P4</b>	0.25	0.25	0.50 [0.59]	0.50 [0.41]	12.9	27.5	2.13	23	11	18.5
PDPP[Py] <sub>2</sub> -T system										
<b>P5</b>	0.00	0.50	1.00 [1.00]	0.00 [0.00]	19.6	54	2.76	24	0	0.0
<b>P6</b>	0.05	0.45	0.90 [0.92]	0.10 [0.08]	18.3	52.7	2.89	24	2	2.7
PDPP[T] <sub>2</sub> -Ph system										
<b>P7</b>	0.00	0.50	1.00 [1.00]	0.00 [0.00]	27.9	46.5	1.67	34	0	0.0
<b>P8</b>	0.05	0.45	0.90 [0.92]	0.10 [0.08]	31.6	74.1	2.35	41	4	2.7
PCDTBT system										
<b>P9</b>	0.00	0.50	1.00 [1.00]	0.00 [0.00]	16.3	36.7	2.25	23	0	0.0
<b>P10</b>	0.05	0.45	0.90 [0.90]	0.10 [0.10]	7.11	15.3	2.15	10	1	3.0

<sup>a</sup>Feed ratio  $f$  of the respective comonomers **a** and **b** as identified in Figures 3 and 4; the feed ratio of  $c$   $f_c$  was kept constant at 0.50. <sup>b</sup>Molar fraction  $\chi$  of repeating unit  $y$  and  $x$  according to feed ratio ( $\chi_f$ ) and calculated from <sup>1</sup>H NMR ( $\chi_{\text{NMR}}$ ) in brackets; see Supporting Information section 5.1 for details. <sup>c</sup>Number-average molecular weight, determined by gel permeation chromatography at 120 °C using 1,2,4-trichlorobenzene as the eluent. <sup>d</sup>Weight-average molecular weight, determined by gel permeation chromatography at 120 °C using 1,2,4-trichlorobenzene as the eluent. <sup>e</sup>Dispersity, determined by gel permeation chromatography at 120 °C using 1,2,4-trichlorobenzene as the eluent. <sup>f</sup>Degree of polymerization estimated from  $M_n$  and the average molecular weight of the polymers repeating unit  $\overline{M}_{\text{RU}}$  (for details see Supporting Information, Table S2). <sup>g</sup>Average number of azide moieties per polymer chain estimated from DP and  $\chi_{\text{RU}}(x)$ . <sup>h</sup>Weight percentage of azido functionalized thiophene in the final polymers calculated by  $\chi_f(x) \times 207.29 \text{ g/mol} / \overline{M}_{\text{RU}}$ , where 207.29 g/mol is the molecular weight of the azido functionalized thiophene moiety and  $\overline{M}_{\text{RU}}$  is the average molecular weight of the polymer's repeating unit given in Supporting Information Table S2.

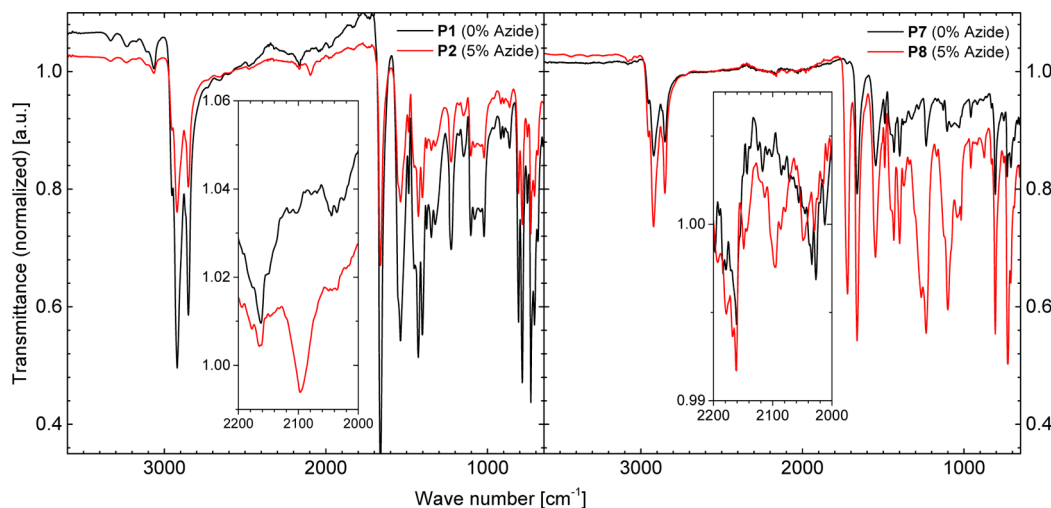


**Figure 5.** Representative infrared spectroscopy of a Stille polycondensation product (PDPP[T]<sub>2</sub>-T system, **P1/P2**) and a Suzuki polycondensation product (PDPP[T]<sub>2</sub>-Ph, **P7/P8**) of the tercopolymers with 5% azide repeating unit content ( $x = 0.1$ , red lines) and their respective nonfunctionalized reference copolymers (black lines). Insets show magnification of the characteristic azide vibration at 2100 cm<sup>-1</sup>. Infrared spectra of the polymer pairs **P5/P6** and **P9/P10** are given in the Supporting Information, Figure S12.

functionalized reference copolymers for reasonably small degrees of azide-functionalization. Assuming full incorporation of the feed ratios of 5 to 25 mol %, the wt % of azide-functionalized thiophene in the final polymers was in the range of only 2.7% to 18.5% for **P2** to **P4**.

The PDPP[T]<sub>2</sub>-T system (**P1–P4**) has the following number-average molecular weights: 36.9 kg mol<sup>-1</sup> for **P1**, 31.6 kg mol<sup>-1</sup> for **P2**, 22.2 kg mol<sup>-1</sup> for **P3**, and 12.9 kg mol<sup>-1</sup> for **P4** corresponding to 0, 5, 10, and 25 mol % of functionalized thiophene, respectively. The decreasing molecular weight with increasing degree of functionalization can be explained by the lower solubility of the tercopolymers with a higher  $x$  fraction due to the small alkyl chains on **5** when compared to the DPP comonomer. As all polymerizations

reached the precipitation limit in pressurized chlorobenzene at 180 °C, higher molecular weights of tercopolymers with high azide content are not accessible in this system. Moreover, the minimum degree of azide functionalization for making the polymers sufficiently insoluble was tested in the series **P1–P4**, and it was found that a molar fraction of 5% content ( $x = 0.1$ ) was sufficient (*vide infra*). Therefore, only 5 mol % functionalization was carried out in further systems (**P5–P10**). The PDPP[Py]<sub>2</sub>-T (**P5/P6**) system which was also prepared using Stille polycondensation shows very comparable molecular weights of 19.6 kg mol<sup>-1</sup> for the nonfunctionalized reference polymer **P5** and 18.3 kg mol<sup>-1</sup> for the polymer **P6** containing 10% azido-functionalized repeating units with almost identical dispersities. Concerning Suzuki polycondensa-

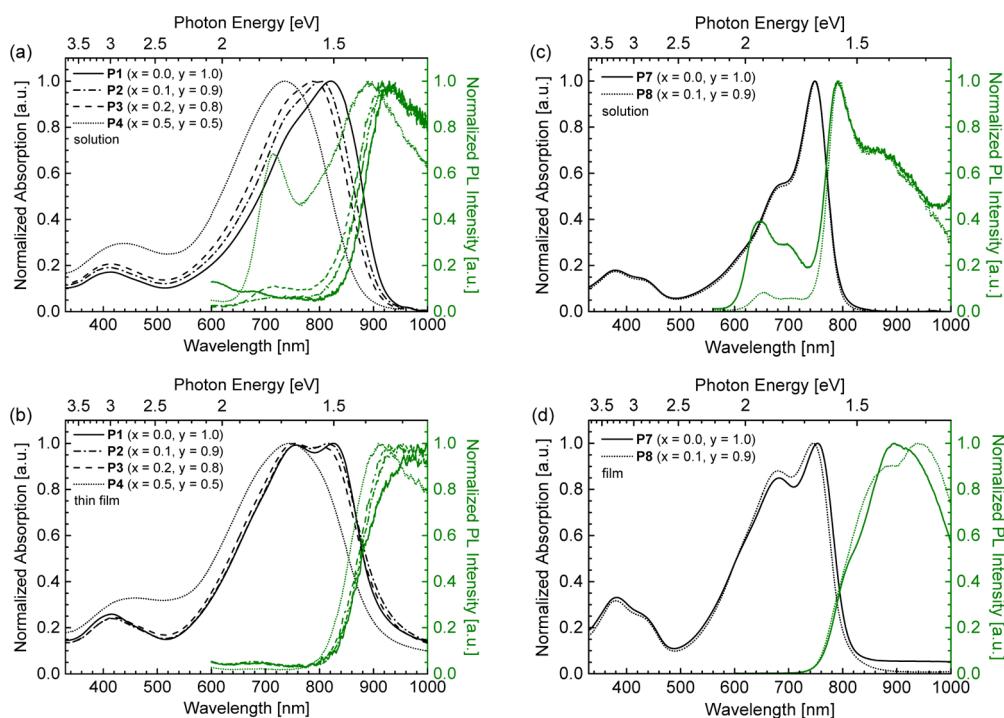


**Figure 6.** Absorption and photoluminescence spectra of cross-linkable tercopolymers compared to their respective nonfunctionalized reference polymers: PDPP[T]<sub>2</sub>-T system **P1–P4** with varying monomer ratios in (a) solution and (b) thin film; PDPP[T]<sub>2</sub>-Ph system **P7/P8** in (c) solution and (d) thin film. See Supporting Information Figure S13 for absorption and photoluminescence spectra of **P5/P6** and **P9/P10**.

tion, the PDPP[T]<sub>2</sub>-Ph system (**P7/P8**) also shows comparable values of 27.9 kg mol<sup>-1</sup> for the nonfunctionalized **P7** and 31.6 kg mol<sup>-1</sup> for the tercopolymer **P8** containing 10% azido-functionalized repeating units. Although the dispersity is a little higher for the functionalized polymer (2.35) than for the reference (1.67), no extreme broadening or tailing can be observed in the GPC elugram; thus, there is no indication for cross-linking under reaction and purification conditions. Only the functionalized PCDTBT polymer **P10** shows a considerably lower molecular weight (7.11 kg mol<sup>-1</sup>) than its reference polymer **P9** (16.3 kg mol<sup>-1</sup>), which is mainly attributed to two different polymerization protocols (i.e., catalyst systems) employed.

**IR Spectroscopy.** In addition to the NMR analysis, the successful azide functionalization was monitored by infrared (IR) spectroscopy of thin polymer films. Comparisons of nonfunctionalized reference polymers and tercopolymers with an azide comonomer content of 10% are shown in Figure 5 and Figure S12 (Supporting Information). A characteristic azide vibration band emerges in all functionalized copolymers at around 2100 cm<sup>-1</sup> showing successful azide functionalization of the polymers.

**Optical Properties.** The optical properties of all the polymers were investigated with respect to absorption as well as photoluminescence (PL) emission. All spectra are shown in Figure 6, and the individual onset wavelengths as well as optical gaps determined from solid state absorption onset are summarized in Table 2. The PDPP[T]<sub>2</sub>-T (**P1–P4**) polymer system with the widest range of degree of functionalization allows to investigate the influence of the tercopolymer ratio *x*:*y* on the optical properties and hence differences in the optical gap as well as aggregation properties. Whereas the spectral nature itself does not change considerably, the solution spectra (Figure 6a) show a small hypsochromic shift of absorption

**Table 2. Electrochemical Properties of Azide-Functionalized Polymers Compared to the Nonfunctionalized Reference Polymers**

polymer	IP <sup>a</sup> [eV]	EA <sup>b</sup> [eV]	E <sub>CV</sub> <sup>c</sup> [eV]	λ <sub>onset</sub> <sup>d</sup> [nm]	E <sub>opt</sub> <sup>e</sup> [eV]
PDPP[T] <sub>2</sub> -T system					
<b>P1</b>	-5.75	-3.69	2.04	928	1.34
<b>P2</b>				938	1.32
<b>P3</b>	-5.69	-3.70	1.99	933	1.33
<b>P4</b>				911	1.36
PDPP[Py] <sub>2</sub> -T system					
<b>P5</b>	-6.08	-3.78	2.30	720	1.72
<b>P6</b>	-6.14	-3.80	2.34	724	1.71
PDPP[T] <sub>2</sub> -Ph system					
<b>P7</b>	-5.72	-3.65	2.07	812	1.53
<b>P8</b>	-5.77	-3.67	2.10	802	1.55
PCDTBT system					
<b>P9</b>	-5.75	-3.50	2.25	665	1.81
<b>P10</b>	-5.79	-3.52	2.27	685	1.86

<sup>a</sup>Ionization potential (HOMO). <sup>b</sup>Electron affinity (LUMO) determined by cyclic voltammetry in thin film. <sup>c</sup>Bandgap determined by cyclic voltammetry in thin film. <sup>d</sup>Absorption onset in film determined therefrom. <sup>e</sup>Optical gap determined therefrom.

offset already at the lowest degree of functionalization with *x* = 0.1 in **P2** (5 mol % azide monomer). This shift only becomes pronounced at a functionalization ratio of *x* = 0.5 in **P4** (25 mol % azide monomer) showing an onset blue-shift of 44 nm (68 meV) and a peak shift of 86 nm (170 meV).

For lower functionalization degrees containing 5–10 mol % azide monomer with *x* = 0.1–0.2 only a very small onset shift of 7–15 nm appears. Whereas the functionalized polymers can still be distinguished from the reference polymers in the solution absorption spectra, the solid state spectra (Figure 6b)

taken of polymer thin films spin-coated on glass are almost identical for low to moderate functionalization degrees. Only **P4** with  $x = 0.5$  shows a distinct small hypsochromic onset shift which is mainly caused by the missing aggregation shoulder. **P2** and **P3** with  $x = 0.1$  and  $x = 0.2$ , respectively, show an identical absorption spectrum compared to the unfunctionalized reference polymer **P1**. This trend is also observable in the photoluminescence of these four polymers. Only **P4** shows a distinctly different emission spectrum in solution and a small hypsochromic shift in the solid state compared to **P1–P3**. For this PDPP system it can therefore be concluded that functionalization degrees up to  $x = 0.2$  can be used without altering any solid state optical properties and that an immense amount of functionalized comonomer **5** has to be used in order to alter the optical properties considerably. It should be emphasized that the repeating unit of the PDPP[**T**]<sub>2</sub>-**T** system comprises three thiophene moieties without addition of the functionalized comonomer **5** and that the addition of another thiophene as third comonomer only partially reduces the DPP content in the tercopolymers, which is the reason for the negligible change in optical properties. We therefore also investigated other systems, for example the system PDPP[**T**]<sub>2</sub>-Ph (**P7/P8**, Figure 6c,d), where the comonomer is not a thiophene but a phenyl moiety, thus decreasing the overall thiophene content in the polymer repeating unit. Taking this one step further, even switching to a different DPP core in the pyridine flanked DPP copolymer system PDPP[Py]<sub>2</sub>-**T** (**P5/P6**, Supporting Information Figure S13a,b) did not lead to a change in optical properties upon introduction of the third monomer. Finally, another low-bandgap polymer system, PCDTBT (**P9/P10**, Supporting Information, Figure S13c,d), was shown not to be influenced by tercopolymerization with **5**. As it was found that sufficient cross-linking in the PDPP[**T**]<sub>2</sub>-**T** system (**P1–P4**) with up to 80% retention of the polymer film (*vide infra*) is possible with as little as 5 mol % azide functionalization, we chose to pursue only this degree of functionalization for all other copolymer systems (**P5–P10**) in order to minimize the influence of chemical changes on the polymer backbone. The absorption as well as emission spectra of the functionalized tercopolymers are compared to the reference polymers in solution (Figure 6c,e,g) and thin film (Figure 6d,f,h), and it can be concluded that a functionalization degree of  $x = 0.1$  has only negligible, if any, influence on the spectral response in the wide range of low-bandgap polymers investigated in this study.

**Electrochemical Properties.** For each polymer system, one functionalized polymer is compared to its unfunctionalized reference polymer. The electrochemical behavior of pairs of similar systems with and without azide functionalization (**P1/P3**, **P5/P6**, **P7/P8**, **P9/P10**) was representatively compared with respect to reversibility as well as redox potentials. The individual cyclic voltammograms are given in the Supporting Information (Figure S11), and the individual energy levels are listed in Table 2 and plotted for comparison in Figure 7. The energy levels were calculated from the redox potentials calibrated against the ferrocene/ferrocenium redox couple using a published procedure taking into account solvent effects.<sup>31</sup> All redox potentials were obtained by cyclic voltammetry on polymer thin films with indium tin oxide (ITO) as the working electrode. Neither the reversibility, the absolute reduction and oxidation potentials, nor the individual voltammograms are influenced by the introduction of the azide-functionalized comonomer. It can hence be concluded that the

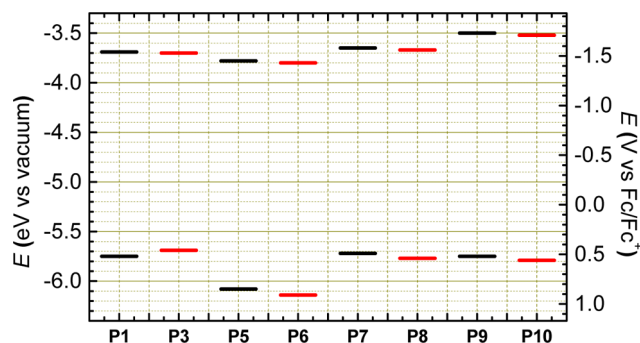


**Figure 7.** Comparison of energy levels of the polymers determined by cyclic voltammetry in thin film. Individual cyclic voltammograms are shown in the Supporting Information, Figure S11.

electrochemical properties in thin film that are dependent on the energy levels of the materials and will not change upon functionalization in the tercopolymers compared to the reference polymers, at least for a functionalization of 5–10 mol %.

**Solvent Resistivity.** In order to check the necessary degree of functionalization to obtain solvent resistivity of the polymers, thin films were cross-linked by UV (254 nm, 1780  $\mu\text{W cm}^{-2}$ ) exposure and then submerged in chloroform for 5 min followed by excessive rinsing with chloroform. The films were dried and analyzed by means of UV/vis absorption and photoluminescence, and the peak intensities were compared to the spectra of the untreated films as obtained after spin-coating. The relative change after UV exposure and after chloroform submerging and rinsing for the polymers **P2**, **P3**, and **P8** is given in Figure 8. Because of the shift of the absorption spectrum in the case of the highly functionalized **P4** polymer (see Figure 6a,b), we chose to omit this polymer in solvent resistivity checks as the application of this polymer is limited by its changed semiconductor properties, even though it has the highest degree of functionalization. Neither absorption nor photoluminescence intensity changes after the films have been exposed to UV radiation, even after 20 min, indicating that the films are stable against UV light and that cross-linking is not negatively influencing the optical properties associated with the conjugated  $\pi$ -system of the polymer backbone. After rinsing the UV-exposed films with chloroform, a functionalization degree of  $x = 10\%$  (5 mol % azide monomer) in the PDPP[**T**]<sub>2</sub>-**T** system (**P2**) requires a minimum UV exposure time of 10–15 min to obtain solvent-resistant films, which retain about 80% of their initial absorption. When the functionalization degree is increased to  $x = 20\%$  (10 mol % azide monomer), the films exhibit onsetting solvent resistivity even after 5 min of UV exposure, again retaining 80% of the absorption. A saturation in solvent resistivity can be obtained after 5–10 min. In the PDPP[**T**]<sub>2</sub>-Ph system a functionalization degree of 5 mol % is enough to obtain full chloroform resistivity after only 1 min of UV exposure. It should be noted that even when saturation in solvent resistivity is reached, the maximal obtainable absorption level was at around 80% of the initial absorption for all cases. Thus, the degree of functionalization influences mainly the onset time required for cross-linking, but for appreciable solvent resistivity 5–10 mol % functionalization is sufficient.

Pictures of a typical experiment outcome is shown in Figure 9, showing two polymer thin films of **P3** spin-coated on a glass substrate with and without prior UV-cross-linking. Interestingly, neither **P6** (PDPP[Py]<sub>2</sub>-**T**) nor **P10** (PCDTBT), both

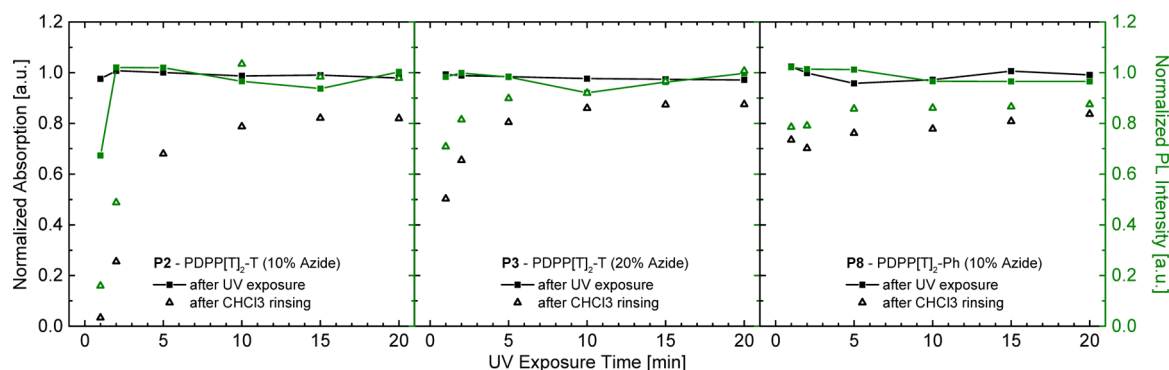


**Figure 8.** Comparison of absorption (black symbols) and photoluminescence (green symbols) for **P2**, **P3**, and **P8** films after UV exposure and chloroform rinsing indicating solvent resistivity for cross-linked films.

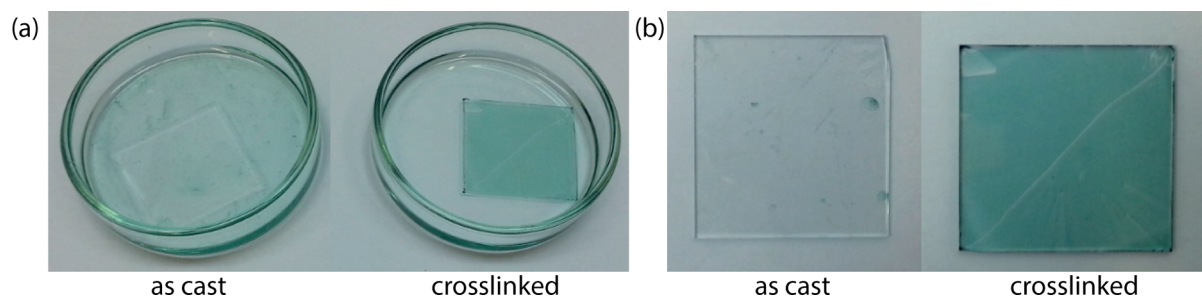


**Figure 9.** Immersion of an as-cast and cross-linked **P3** thin film on glass substrates: (a) immersion in chloroform (the green hue in the solution with the cross-linked sample is due to refraction of the green polymer thin film in the glass of the Petri dish); (b) samples after rinsing with chloroform.

with  $x = 10\%$  (5 mol % azide functionalization), could be cross-linked to a degree where resistivity against chloroform is obtained. This could be attributed to the high intrinsic solubility of those polymers. The pyridine flanked PDPP-[Py]<sub>2</sub>-M<sub>co</sub> system, for example, is even soluble in hexane as has been previously reported.<sup>27</sup>

It can therefore be expected that chloroform provides enough solubility even for cross-linked systems. This also indicates that the degree of cross-linking should be tuned depending on the solubility properties of the concerned polymer system.

**Solid State Structure.** In order to elucidate the influence of cross-linking on the solid state structure of the polymers in thin films, i.e., crystallinity and the alignment with the substrate, we have measured grazing incidence wide-angle X-ray scattering (GIWAXS) for the three different systems (**P1/P2**, **P5/P6**, and **P7/P8**) comparing the unfunctionalized reference polymers to their functionalized, cross-linked tercopolymers. The individual spacing  $d$  and coherence length  $\zeta$  values for the different crystalline directions (along the alkyl-stacked lamella and the  $\pi$ - $\pi$  stacked faces) are summarized in Table 3. As an example, Figure 10 shows a comparison of unfunctionalized **P1** to the azido-functionalized **P2** (PDPP[T]<sub>2</sub>-T system) in both as-cast as well as UV-exposed and annealed films. UV exposure was performed under ambient conditions; annealing was carried out at 250 °C under an inert atmosphere. Whereas in **P1** a significant increase in the degree of edge-on alignment can be observed after thermal annealing, showing up to the fourth-order reflection of the alkyl-stacking peak (labeled  $h00$ ) and very large coherence lengths (25.2 nm) in both the in-plane and out-of-plane direction, annealing of **P2** only leads to a moderate increase of edge-on crystallinity.

**Table 3. GIWAXS Peak Analysis of Neat Polymer Thin Films for Alkyl,  $\pi$ - $\pi$ , and Backbone Stacking**

polymer	$T^a$	$d_{\text{alkyl}}^b$ [nm]	$\zeta_{\text{alkyl}}^{c,f}$ [nm]	$d_{\pi-\pi}^d$ [nm]	$\zeta_{\pi-\pi}^{e,f}$ [nm]
<b>P1</b>	as cast	1.98(4)	6.3(8)	0.401(3)	3.5(1)
<b>P1</b>	250 °C	2.01(4)	25.2(3)	0.402(1)	4.27(6)
<b>P2</b>	as cast	1.89(2)	4.5(2)	0.380(1)	3.2(2)
<b>P2</b>	250 °C	2.00(5)	13.5(1)	0.395(2)	4.0(3)
<b>P5</b>	as cast	1.98(3)	3.36(7)	0.393(1)	3.4(2)
<b>P5</b>	250 °C	2.03(5)	25.1(2)	0.391(0)	3.9(1)
<b>P6</b>	as cast	1.89(0)	3.94(0)		
<b>P6</b>	250 °C	1.98(5)	14.0(1)	0.393(0)	2.74(2)
<b>P7</b>	as cast	1.94(3)	8.32(3)	0.382(2)	3.3(2)
<b>P7</b>	250 °C	1.95(3)	16.2(1)	0.406(5)	3.43(3)
<b>P8</b>	as cast	1.89(4)	5.85(6)	0.402(2)	2.86(7)
<b>P8</b>	250 °C	1.95(2)	15.6(2)	0.412(0)	3.58(4)

<sup>a</sup>Annealing process. <sup>b</sup>Alkyl stacking spacing. <sup>c</sup>Alkyl stacking coherence length (determined from (100) peak in out-of-plane direction). <sup>d</sup> $\pi$ - $\pi$  stacking spacing. <sup>e</sup> $\pi$ - $\pi$  stacking coherence length (determined from 1st order  $\pi$ - $\pi$  stacking). <sup>f</sup>The crystal coherence length  $\zeta$  gives information about the distance over which order is maintained and is defined as  $\zeta = 2\pi/\text{fwhm}$ , where fwhm is the full width at half-maximum of the first-order lamellar stacking or  $\pi$ - $\pi$  stacking peak, respectively. It is related to the Scherrer equation, which connects the width of a peak to the crystal size.

While edge-on crystallinity is dominant in **P1**, there is a significant population of face-on stacking with much larger coherence lengths evident by the quite sharp alkyl-stacking reflections in-plane. Comparisons for the other polymer systems (**P5/P6**, **P7/P8**) are given in Supporting Information Figures S14 and S15, respectively. Similar behavior can be observed in the pyridine flanked PDPP[Py]<sub>2</sub>-T system when comparing unfunctionalized **P5** to functionalized **P6** (see

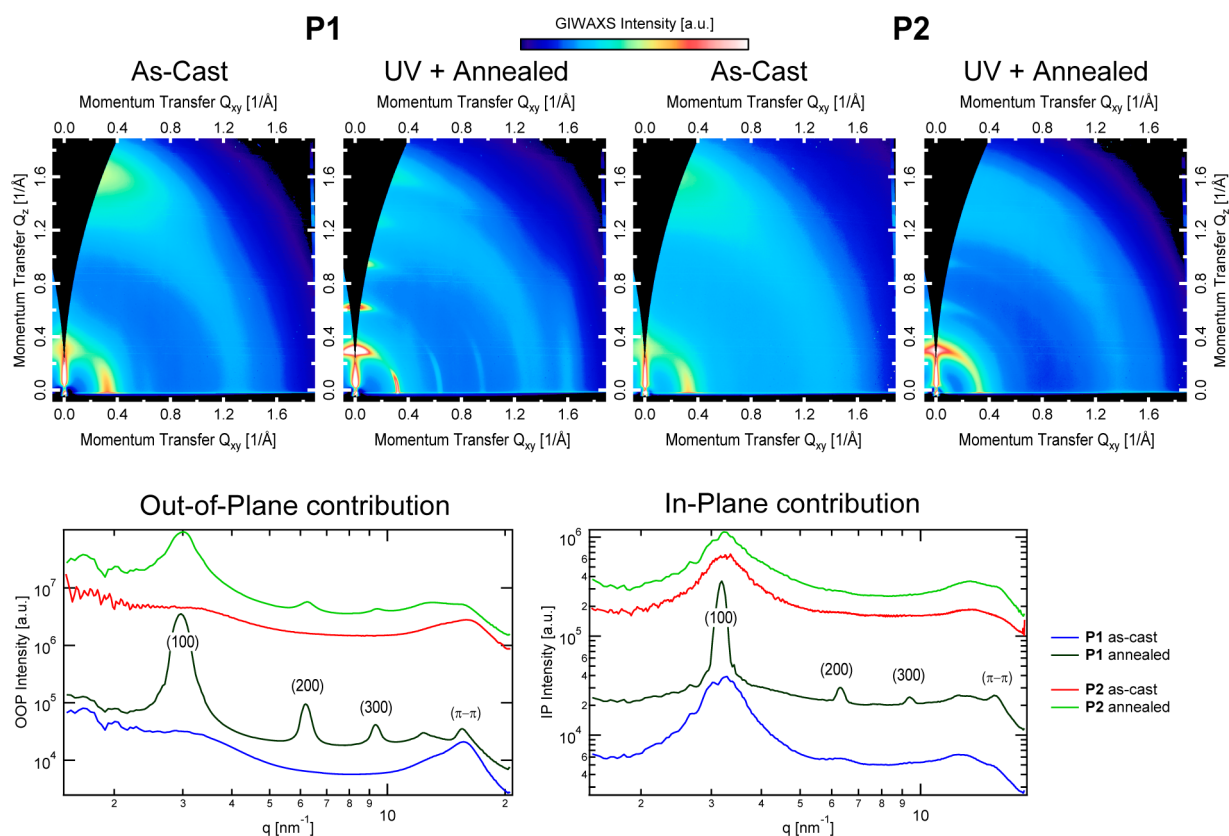


**Figure 10.** GIWAXS scatter patterns of neat unfunctionalized (P1) and azide-functionalized (P2) PDPP[T]<sub>2</sub>-T polymer thin films. Both the reference P1 and the P2 film were exposed to UV light before thermal annealing.

**Table 4.** GIWAXS Peak Analysis of Polymer:PC<sub>70</sub>BM Blend Systems for Alkyl,  $\pi$ - $\pi$ , and Backbone Stacking

blend	T <sup>a</sup>	d <sub>alkyl</sub> <sup>b</sup> [nm]	$\zeta$ <sub>alkyl</sub> <sup>c,h</sup> [nm]	d <sub><math>\pi</math>-<math>\pi</math></sub> <sup>d</sup> [nm]	$\zeta$ <sub><math>\pi</math>-<math>\pi</math></sub> <sup>e,h</sup> [nm]	d <sub>bb</sub> <sup>f</sup> [nm]	$\zeta$ <sub>bb</sub> <sup>g,h</sup> [nm]
P1:PC <sub>70</sub> BM	as cast	1.97(3)	7.8(1)	0.380(2)	1.7(1)	1.56(1)	5.3(5)
P1:PC <sub>70</sub> BM	200 °C	2.05(4)	20.0(2)	0.358(7)	2.4(1)	1.43(1)	3.8(3)
P2:PC <sub>70</sub> BM	as cast	1.95(2)	12(1)	0.381(1)	1.6(1)	1.53(5)	3.5(6)
P2:PC <sub>70</sub> BM	200 °C	1.94(1)	7.47(9)	0.381(1)	1.6(1)	1.46(3)	3.5(6)
P5:PC <sub>70</sub> BM	as cast	1.89(7)	4.5(2)	0.359(1)	3.0(2)		
P5:PC <sub>70</sub> BM	200 °C	2.01(6)	15.5(1)	0.389(1)	2.1(1)		
P6:PC <sub>70</sub> BM	as cast	1.84(6)	6.7(6)	0.360(2)	2.9(3)		
P6:PC <sub>70</sub> BM	200 °C	1.90(1)	5.06(0)	0.369(1)	1.8(1)		
P7:PC <sub>70</sub> BM	as cast	1.95(3)	9.3(1)	0.393(1)	2.2(1)	1.54(1)	6(1)
P7:PC <sub>70</sub> BM	200 °C	1.95(4)	9.1(1)	0.391(1)	2.3(1)	1.50(1)	5.8(6)
P8:PC <sub>70</sub> BM	as cast	1.91(1)	7.58(8)	0.388(2)	1.6(1)	1.54(1)	5.2(7)
P8:PC <sub>70</sub> BM	200 °C	1.91(1)	7.2(1)	0.397(0)	6(1)	1.47(2)	2.9(5)

<sup>a</sup>Annealing process. <sup>b</sup>Alkyl stacking spacing. <sup>c</sup>Alkyl stacking coherence length (determined from (100) peak in out-of-plane direction). <sup>d</sup> $\pi$ - $\pi$  stacking spacing. <sup>e</sup> $\pi$ - $\pi$  stacking coherence length (determined from first-order  $\pi$ - $\pi$  stacking). <sup>f</sup>Backbone stacking spacing. <sup>g</sup>Backbone stacking coherence length (determined from first-order backbone stacking in in-plane direction). <sup>h</sup>The crystal coherence length  $\zeta$  gives information about the distance over which order is maintained and is defined as  $\zeta = 2\pi/\text{fwhm}$ , where fwhm is the full width at half-maximum of the first-order lamellar stacking or  $\pi$ - $\pi$  stacking peak, respectively. It is related to the Scherrer equation, which connects the width of a peak to the crystal size.

Supporting Information Figure S14). P5 shows a considerable increase in crystallinity and well-aligned films with several orders of alkyl spacing present both out-of-plane and in-plane after thermal annealing. Again, the P6 film is somewhat influenced by annealing but to a much smaller extent, showing first-order peaks and considerably smaller coherence lengths (Table 3). Finally, in the PDPP[T]<sub>2</sub>-Ph system comparing unfunctionalized P7 to functionalized P8 (see Supporting Information, Figure S15) cross-linking of P8 has much less of an effect on both crystallinity and degree of alignment. Both polymers show a strongly enhanced crystallinity and edge-on

alignment after thermal annealing, independent of the azide-content and cross-linking. In fact, P8 shows a clearer edge-on conformation than the reference P7 as indicated by the complete absence of the alkyl spacing peaks in the in-plane direction in P8 after annealing. This points to face on orientation in these films being hindered by cross-linking. The backbone spacing  $d_{bb}$  and the respective backbone spacing coherence length  $\zeta_{bb}$  could only be observed in P7 after annealing and was found to be 1.53(0) nm and 10.0(5) nm, respectively.

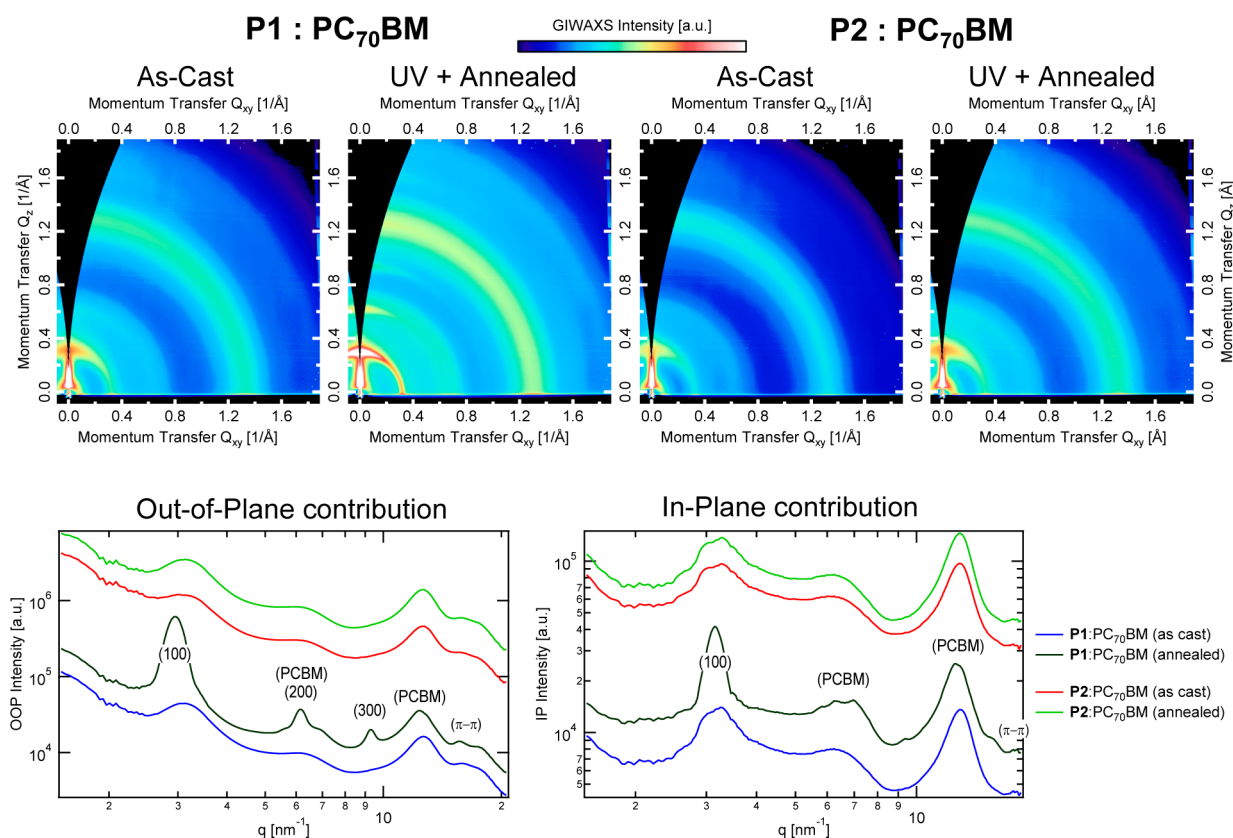


**Figure 11.** GIWAXS scatter patterns of unfunctionalized (P1) and azide-functionalized (P2) PDPP[T]<sub>2</sub>-T polymer:PC<sub>70</sub>BM blends. Both the reference P1 and the P2 film were exposed to UV light before thermal annealing. Comparisons for different polymer systems (P5/P6, P7/P8) are given in Supporting Information Figures S16 and S17, respectively.

**Blends.** Since the importance of cross-linking a low-bandgap polymer is usually discussed as a route to stabilize the morphology of blends with fullerene derivatives as in solar cell applications, we tested the potential of our concept in similar blends as well. For this, we have selected the polymer pairs P1/P2, P5/P6, and P7/P8 and tested the cross-linking conditions. From our experience with the non-functionalized reference polymers P1, P5, and P7, the polymer:PC<sub>70</sub>BM blend morphology is much more favorable for solar cell applications when DIO is used as a solvent additive. Hence, we chose to add DIO to the blends investigated in GIWAXS. Additionally, we have also performed GIWAXS measurements on polymer/fullerene blends before and after cross-linking/annealing. 2D GIWAXS patterns were taken for the as cast films as well as for films that were exposed to UV radiation followed by thermal annealing at 200 °C for 15 min in an inert atmosphere. The individual spacings  $d$  and coherence lengths  $\zeta$  along the different crystalline directions (alkyl,  $\pi$ - $\pi$ , and backbone) are summarized in Table 4. Figure 11 shows the 2D scattering patterns for the PDPP[T]<sub>2</sub>-T system comparing unfunctionalized P1 with functionalized P2 ( $x = 0.1$ ) as a typical example. Whereas the as-cast blend films show almost identical scattering in both in-plane and out-of-plane direction, upon annealing the P1 blend shows a distinct increase in crystallinity with second- and third-order lamellar stacking peaks appearing in the out-of-plane direction. Also, the in-plane scattering shows a higher intensity and a narrower peak for the first-order lamellar stacking peak, indicating a larger crystal coherence length in the annealed sample. These annealing effects are absent in the cross-linked P2 blend after

thermal annealing, indicating a lower chain mobility which hinders improved packing upon annealing. The same effect can also be observed in the blends employing the PDPP[Py]<sub>2</sub>-T system (see Supporting Information, Figure S16). Again the unfunctionalized P5 blend shows an increasing crystallinity and exhibits distinct second-order peaks upon annealing which are lacking in the cross-linked and annealed P6 blend. In fact, the scattering of the annealed P6 blend is identical to the as-cast P6 blend and the as-cast P5 blend, indicating successful cross-linking and chain immobilization in this system. Interestingly, the PDPP[T]<sub>2</sub>-Ph system does not show any differences after thermal annealing in the unfunctionalized P7 blend as well as in the tercopolymer P8 blend having 5 mol % azide functionalization (see Supporting Information Figure S17).

We want to highlight a noticeable peculiarity apart from any cross-linking questions, namely, the fact that for the thiophene flanked PDPP[T]<sub>2</sub>-T (P1/P2) and PDPP[T]<sub>2</sub>-Ph (P7/P8) systems we consistently observe backbone stacking peaks when blended with PC<sub>70</sub>BM (Table 4), which are not observable in the corresponding neat polymer thin films (Table 3), especially in P1, P2, and P8. This is suggesting a PC<sub>70</sub>BM-influenced packing in the blends.

**OFET.** The performance of the polymers in organic field effect transistors (OFET) was representatively investigated to study the influence of azide incorporation on the PDPP[T]<sub>2</sub>-T system using the unfunctionalized P1 as a reference and P3 exhibiting a functionalization degree of  $x = 0.2$  (10 mol % azide monomer). OFET devices were prepared in a bottom gate/bottom contact (BGBC) configuration. In order to get a clear picture about the influence of incorporation of a third

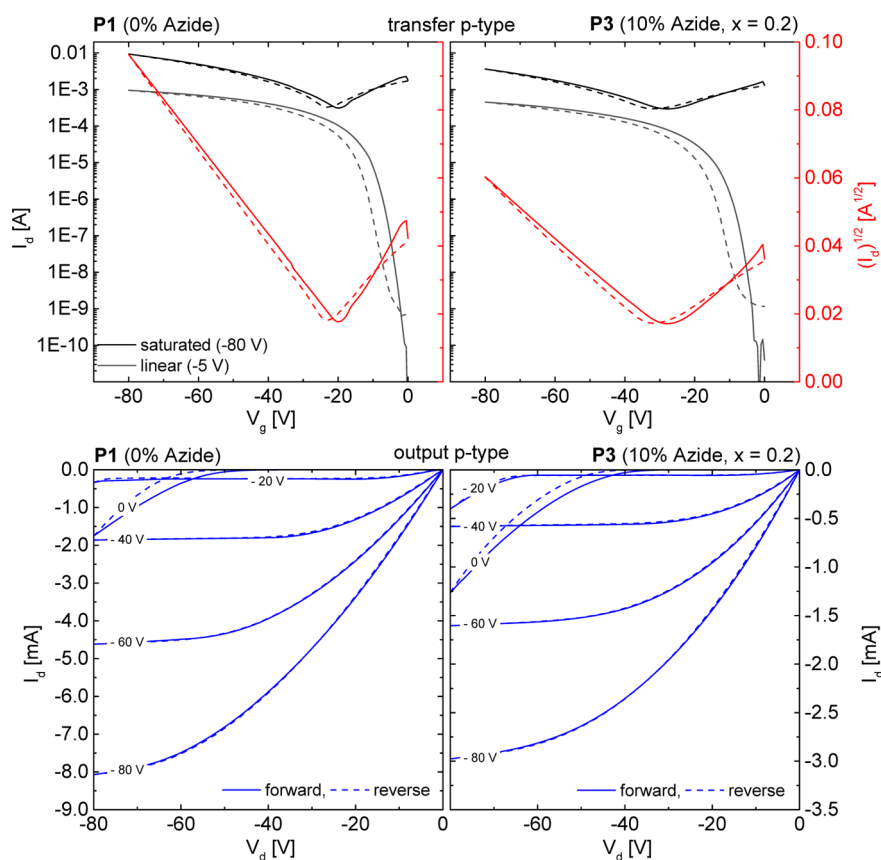


**Figure 12.** OFET p-type transfer and output  $I$ – $V$  characteristics after annealing at 250 °C for 15 min of the nonfunctionalized strictly alternating PDPP[T]<sub>2</sub>-T **P1** and the tercopolymer containing 10% azide-functionalized repeating units **P3**. Solid and dashed lines represent the forward and reverse scans in all graphs, respectively. The voltages given in the legend of the output characteristics are the applied gate voltages.

comonomer into this copolymer system, neither of the films has been exposed to UV radiation for cross-linking before characterizing the transistors. The mobility was averaged over at least three individual devices. Both polymers show an ambipolar behavior, although the p-channel is much more dominant. Transfer and output  $I$ – $V$  characteristics for p-channel operation are shown in Figure 12. In the as-cast films the hole mobility was  $\mu_h = 0.28 \pm 0.17 \text{ cm}^2 \text{ V}^{-1} \text{ s}^{-1}$  for **P1** compared to  $\mu_h = 0.04 \pm 0.01 \text{ cm}^2 \text{ V}^{-1} \text{ s}^{-1}$  in the case of the functionalized derivative **P3**. Upon annealing, the mobilities increased considerably to  $\mu_h(\text{P1}) = 0.45 \pm 0.02 \text{ cm}^2 \text{ V}^{-1} \text{ s}^{-1}$  and  $\mu_h(\text{P3}) = 0.19 \pm 0.03 \text{ cm}^2 \text{ V}^{-1} \text{ s}^{-1}$ , respectively. Even though the final mobility of the azide-functionalized tercopolymer **P3** is a little lower than that of the reference polymer **P1** after annealing, it is important to note that mobilities in the same order of magnitude are accessible using this tercopolymerization approach and that even a moderate azide-functionalization of 10 mol % with  $x = 0.2$  does obviously not drastically limit the thermal annealing options of non-UV-cross-linked films, allowing good postprocessing opportunities via thermal annealing which is common for organic semiconducting materials. The same holds true for n-type operation. Transfer and output characteristics for n-channel operation are shown in the Supporting Information, Figure S18. The transistors exhibit a significant threshold voltage of 50 V, and hence output in the n-channel can only be observed for gate voltages as high as 60–80 V. The electron mobilities are  $\mu_e(\text{P1}) = 0.14 \pm 0.01 \text{ cm}^2 \text{ V}^{-1} \text{ s}^{-1}$  and  $\mu_e(\text{P3}) = 0.06 \pm 0.01 \text{ cm}^2 \text{ V}^{-1} \text{ s}^{-1}$ .

## CONCLUSION

In conclusion, we have shown a new and highly modular concept for the synthesis of photo-cross-linkable semiconducting polymers to obtain both solvent-resistant films as well as thermally stable solid state packing and morphologies in thin films of neat polymers and in PC<sub>70</sub>BM blends after photo-cross-linking. The synthetic effort was kept low by the universal use of a common azido-functionalized thiophene comonomer in four different copolymer systems without influencing the optical and electrochemical properties of the polymers. Successful incorporation of azide moieties in the functionalized tercopolymers was proven by infrared and NMR spectroscopy. The introduction of the additional monomer containing the azide moiety did not considerably alter the optical or electrical properties in thin films and devices as demonstrated in an organic field effect transistor for a degree of functionalization up to  $x = 0.2$  (10 mol % azide monomer). We anticipate that this cross-linking approach will provide an easily accessible route toward a variety of inherently cross-linkable semiconductor polymers using a single universal cross-linkable unit without the necessity of the addition of low molecular weight cross-linking agents.

## EXPERIMENTAL SECTION

**Materials and Methods.** All reagents were used without further purification unless otherwise noted. Microwave reactions were conducted in sealed containers using a Biotage Initiator Eight+ microwave. <sup>1</sup>H NMR (300 MHz) spectra of monomers were recorded on a Bruker AC 300 spectrometer. All polymer <sup>1</sup>H NMR spectra were recorded on a Varian INOVA 300 spectrometer at 393 K in 1,1,2,2-

tetrachloroethane (TCE) as solvent. The  $^1\text{H}$  spectra were referenced internally by using the residual solvent resonances. Deuterated solvents were obtained from Deutero. Gel permeation chromatography (GPC) analysis was carried out on an Agilent (Polymer Laboratories Ltd.) PL-GPC 220 high temperature chromatographic unit equipped with DP, RI, and LS ( $15^\circ$  and  $90^\circ$ ) detectors and three linear mixed bed columns of PLgel 13  $\mu\text{m}$  (Olexis) with a linear MW operating range: 500–15 000 000  $\text{g mol}^{-1}$ . GPC analysis was performed at  $150^\circ\text{C}$  using 1,2,4-trichlorobenzene as the mobile phase. The samples were prepared by dissolving the polymer (0.1 wt %) in the mobile phase solvent in an external oven and the solutions were run without filtration. The molecular weights of the samples were referenced to linear polystyrene ( $M_w = 162\text{--}6\,000\,000\ \text{g mol}^{-1}$ ,  $K = 12.100$ , and  $\text{Alpha} = 0.707$ ) and were not corrected with  $K$  and  $\text{Alpha}$  values for the measured sample. Cyclic voltammetry was performed under moisture- and oxygen-free conditions using a 0.1 M tetra-*n*-butylammonium hexafluorophosphate in acetonitrile electrolyte solution. A standard three-electrode assembly connected to a potentiostat (model 263A, EG&G Princeton Applied Research) was used at a scanning rate of  $100\ \text{mV s}^{-1}$ . The working electrode was a  $10\ \Omega/\square$  ITO-coated glass substrate. The polymers were spin-coated onto the ITO substrates from chloroform at 3 mg/mL and 1500 rpm to obtain thicknesses of 10–20 nm. A platinum wire in acetonitrile was used as counter electrode, and the quasi-reference electrode consisted of an Ag wire in an  $\text{AgNO}_3/\text{acetonitrile}$  solution (0.1 M). The measurements were calibrated with an external ferrocene/ferrocenium standard; IP and EA values were calculated considering the solvent effects as per a published procedure<sup>31</sup> using eqs 1 and 2 where the workfunction of  $\text{Fc}/\text{Fc}^+$  is taken to be  $-5.23\ \text{eV}$ . The reduction half-step potential  $E_{1/2}^{\text{red}}$  (vs  $\text{Fc}/\text{Fc}^+$ ) is negative whereas the oxidation half-step potential  $E_{1/2}^{\text{ox}}$  (vs  $\text{Fc}/\text{Fc}^+$ ) is positive.

$$\text{EA} \approx -5.23\ \text{eV} - E_{1/2}^{\text{red}}\ (\text{vs Fc}/\text{Fc}^+) \quad (1)$$

$$\text{IP} \approx -5.23\ \text{eV} - E_{1/2}^{\text{ox}}\ (\text{vs Fc}/\text{Fc}^+) \quad (2)$$

Absorption measurements were carried out on a JASCO V-670 spectrophotometer. Photoluminescence measurements were carried out on a JASCO FP-8600 spectrofluorometer; excitation wavelengths were chosen at the maximum of the transition around 430 nm for all samples. Optical properties in solution were measured in chloroform at a concentration of 0.01 mg/mL and a path length of 10 mm; films were spin-coated onto glass slides from a 7 mg/mL chloroform solution at 1500 rpm. Solutions for spin-coating were prepared by dissolving the polymer in chloroform at the given concentration and stirring at  $55^\circ\text{C}$  for 8 h. Cross-linking by UV exposure for the resistivity experiments was performed using a benchtop UV lamp operating at 254 nm with an intensity of  $1780\ \mu\text{W cm}^{-2}$ ; cross-linking for the GIWAXS experiments was performed using a commercial system (Light Hammer 6, Fusion Systems Inc., 200–450 nm,  $200\ \text{W cm}^{-2}$  on a LC6 benchtop conveyor operating at 3.5 cm/s).

**GIWAXS.** The GIWAXS measurements were conducted at the SAXS/WAXS beamline of the Australian Synchrotron.<sup>32</sup> Neat polymer films were spin-coated from chloroform onto an octyltrichlorosilane/ $\text{SiO}_2$  modified silicon wafer from a 6 mg  $\text{mL}^{-1}$  solution at 2000 rpm. Blend samples were prepared by spin-coating polymer:PC<sub>70</sub>BM blends (ratio 1:2) from chloroform at a total concentration of 18 mg/mL with 2 vol % 1,8-diiodooctane (DIO) onto an  $\text{MoO}_3$  (15 nm) modified silicon wafer at 2000 rpm. After spin-coating the films were immediately put under ultrahigh vacuum (base pressure  $10^{-7}$  mbar) in order to evaporate remaining DIO. Highly collimated 9 keV X-rays were calibrated to be at a tilt angle of  $0 \pm 0.01^\circ$  when parallel to the surface of each sample by use of a silicon crystal analyzer. A Dectris Pilatus 1M detector collected 2D scattering patterns, including those shown in Figures 10 and 11. Each scattering pattern was tiled together from three 1 s images with the detector slightly moved between exposures, such that the resulting image removes gaps between the detector modules. The sample-to-detector distance was measured using a silver behenate scattering standard. Data were analyzed using a

modified version of the NIKA small-angle scattering analysis package.<sup>33</sup>

**Organic Thin Film Transistors.** Substrates in bottom gate/bottom contact configuration were bought from Fraunhofer IPMS (OFET Gen. 4). Heavily n-doped silicon (doping at wafer surface:  $n \sim 3 \times 10^{17}\ \text{cm}^{-3}$ ) was used as substrate and gate electrode. Thermally grown silicon oxide ( $230 \pm 10\ \text{nm}$ ) was used as the gate dielectric. Gold electrodes (30 on 10 nm ITO as adhesion layer) were used as source and drain contacts. The channel width was 10 mm for all devices and channel lengths of 10 and 20  $\mu\text{m}$  were used. The substrates were cleaned subsequently in acetone and 2-propanol in an ultrasonic bath for 10 min each. Treatment in an ozone oven at  $50^\circ\text{C}$  for 20 min was followed by immersion in a 1 wt % solution of octadecyltrichlorosilane in toluene at  $60^\circ\text{C}$  for 60 min. After rinsing with toluene and 2-propanol the substrates were dried in a nitrogen stream, and the polymer was spin-coated from a 6 mg/mL chloroform solution at 2000 rpm under ambient conditions. Devices were measured in a nitrogen atmosphere using an Agilent B1500 Semiconductor Parameter Analyzer. The devices were annealed in a nitrogen atmosphere at a maximum of 0.9 ppm of  $\text{O}_2$  for 15 min consecutively at the temperatures given in the main text. Mobilities were calculated from the slopes in the  $(I_d)^{0.5}\text{--}V_g$  plots in the saturation regime using eq 3, where  $I_d$  is the drain current,  $W$  the channel width,  $L$  the channel length,  $C_i$  the capacitance,  $V_g$  the gate voltage, and  $V_T$  the threshold voltage.

$$I_d \approx \frac{W}{2L} C_i \mu (V_g - V_T)^2 \quad (3)$$

## ■ ASSOCIATED CONTENT

### 📄 Supporting Information

The Supporting Information is available free of charge on the ACS Publications website at DOI: 10.1021/acs.macromol.5b02659.

Monomer syntheses, characterization of monomers, polymer syntheses, detailed characterization of polymers including GPC, cyclic voltammetry, and additional GIWAXS data (PDF)

## ■ AUTHOR INFORMATION

### Corresponding Author

\*E-mail mukundan.thelakkat@uni-bayreuth.de (M.T.).

### Notes

The authors declare no competing financial interest.

## ■ ACKNOWLEDGMENTS

We thank Christina Saller (Universität Bayreuth) for providing the unfunctionalized PCDTBT as reference material. We acknowledge financial support from the Bavarian State Ministry of the Environment and Consumer Protection (Umwelt NanoTech) and the Bavarian State Ministry of Education, Science and the Arts (Solar technologies go hybrid). C.J.M. thanks the Fonds der Chemischen Industrie for funding the PhD with a Kekulé scholarship. C.J.M. and T.K. kindly acknowledge scholarships from the German National Academic Foundation and support from the Elitenetzwerk Bayern (ENB), Macromolecular Science. C.R.M. acknowledges support from the Australian Research Council (DP130102616). This research was undertaken in part on the SAXS/WAXS beamline at the Australian Synchrotron, Victoria, Australia.<sup>32</sup>

## ■ REFERENCES

(1) Halls, J. J. M.; Walsh, C. A.; Greenham, N.; Marseglia, E. A.; Friend, R. H.; Moratti, S. C.; Holmes, A. B. Efficient photodiodes from interpenetrating polymer networks. *Nature* **1995**, *376*, 498.

- (2) Yu, G.; Gao, J.; Hummelen, J. C.; Wudl, F.; Heeger, A. J. Polymer Photovoltaic Cells: Enhanced Efficiencies via a Network of Internal Donor-Acceptor Heterojunctions. *Science* **1995**, *270*, 1789.
- (3) Liu, Y.; Zhao, J.; Li, Z.; Mu, C.; Ma, W.; Hu, H.; Jiang, K.; Lin, H.; Ade, H.; Yan, H. Aggregation and morphology control enables multiple cases of high-efficiency polymer solar cells. *Nat. Commun.* **2014**, *5*, 5293.
- (4) Hösel, M.; Søndergaard, R. R.; Jørgensen, M.; Krebs, F. C. Fast Inline Roll-to-Roll Printing for Indium-Tin-Oxide-Free Polymer Solar Cells Using Automatic Registration. *Energy Technology* **2013**, *1*, 102.
- (5) Griffini, G.; Douglas, J. D.; Piliago, C.; Holcombe, T. W.; Turri, S.; Frechet, J. M.; Mynar, J. L. Long-term thermal stability of high-efficiency polymer solar cells based on photocrosslinkable donor-acceptor conjugated polymers. *Adv. Mater.* **2011**, *23*, 1660.
- (6) Rumer, J. W.; McCulloch, I. Organic photovoltaics: Crosslinking for optimal morphology and stability. *Mater. Today* **2015**, *18*, 425.
- (7) Carle, J. E.; Andreasen, B.; Tromholt, T.; Madsen, M. V.; Norrman, K.; Jørgensen, M.; Krebs, F. C. Comparative studies of photochemical cross-linking methods for stabilizing the bulk heterojunction morphology in polymer solar cells. *J. Mater. Chem.* **2012**, *22*, 24417.
- (8) Wantz, G.; Derue, L.; Dautel, O.; Rivaton, A.; Hudhomme, P.; Dagon-Lartigau, C. Stabilizing polymer-based bulk heterojunction solar cells via crosslinking. *Polym. Int.* **2014**, *63*, 1346.
- (9) Chen, M.-R.; Fan, C.-C.; Andersen, T. R.; Dam, H. F.; Fu, W.-F.; Lin, Y.-Z.; Bundgaard, E.; Krebs, F. C.; Zhan, X.-W.; Chen, H.-Z. Solvent-resistant small molecule solar cells by roll-to-roll fabrication via introduction of azide cross-linkable group. *Synth. Met.* **2014**, *195*, 299.
- (10) Kim, B. J.; Miyamoto, Y.; Ma, B.; Fréchet, J. M. J. Photocrosslinkable Polythiophenes for Efficient, Thermally Stable, Organic Photovoltaics. *Adv. Funct. Mater.* **2009**, *19*, 2273.
- (11) Kim, H. J.; Han, A. R.; Cho, C.-H.; Kang, H.; Cho, H.-H.; Lee, M. Y.; Fréchet, J. M. J.; Oh, J. H.; Kim, B. J. Solvent-Resistant Organic Transistors and Thermally Stable Organic Photovoltaics Based on Cross-linkable Conjugated Polymers. *Chem. Mater.* **2012**, *24*, 215.
- (12) Nam, C.-Y.; Qin, Y.; Park, Y. S.; Hlaing, H.; Lu, X.; Ocko, B. M.; Black, C. T.; Grubbs, R. B. Photo-Cross-Linkable Azide-Functionalized Polythiophene for Thermally Stable Bulk Heterojunction Solar Cells. *Macromolecules* **2012**, *45*, 2338.
- (13) Murray, K. A.; Holmes, A. B.; Moratti, S. C.; Friend, R. H. The synthesis and crosslinking of substituted regioregular polythiophenes. *Synth. Met.* **1996**, *76*, 161.
- (14) Murray, K. A.; Holmes, A. B.; Moratti, S. C. Rumbles, G. Conformational changes in regioregular polythiophenes due to crosslinking. *J. Mater. Chem.* **1999**, *9*, 2109.
- (15) Png, R. Q.; Chia, P. J.; Tang, J. C.; Liu, B.; Sivaramakrishnan, S.; Zhou, M.; Khong, S. H.; Chan, H. S.; Burroughes, J. H.; Chua, L. L.; Friend, R. H.; Ho, P. K. High-performance polymer semiconducting heterostructure devices by nitrene-mediated photocrosslinking of alkyl side chains. *Nat. Mater.* **2010**, *9*, 152.
- (16) Liu, B.; Png, R. Q.; Zhao, L. H.; Chua, L. L.; Friend, R. H.; Ho, P. K. High internal quantum efficiency in fullerene solar cells based on crosslinked polymer donor networks. *Nat. Commun.* **2012**, *3*, 1321.
- (17) Davis, A. R.; Carter, K. R. Controlling Optoelectronic Behavior in Poly(fluorene) Networks Using Thiol–Ene Photo-Click Chemistry. *Macromolecules* **2015**, *48*, 1711.
- (18) Tao, C.; Aljada, M.; Shaw, P. E.; Lee, K. H.; Cavaye, H.; Balfour, M. N.; Borthwick, R. J.; James, M.; Burn, P. L.; Gentle, I. R.; Meredith, P. Controlling Hierarchy in Solution-processed Polymer Solar Cells Based on Crosslinked P3HT. *Adv. Energy Mater.* **2013**, *3*, 105.
- (19) Neubig, A.; Thelakkat, M. Random vs. alternating donor-acceptor copolymers: A comparative study of absorption and field effect mobility. *Polymer* **2014**, *55*, 2621.
- (20) Karolewski, A.; Neubig, A.; Thelakkat, M.; Kummel, S. Optical absorption in donor-acceptor polymers—alternating vs. random. *Phys. Chem. Chem. Phys.* **2013**, *15*, 20016.
- (21) Bäuerle, P.; Würthner, F.; Heid, S. Einfache Synthese von 3-( $\omega$ -Halogenalkyl)thiophenen als Grundbausteinen für funktionalisierte Thiophene und Polythiophene. *Angew. Chem.* **1990**, *102*, 414.
- (22) Buckel, F.; Persson, P.; Effenberger, F. Synthesis of Functionalized Long-Chain Thiols and Thiophenols for the Formation of Self-Assembled Monolayers on Gold. *Synthesis* **1999**, *1999*, 953.
- (23) Zhai, L.; Pilston, R. L.; Zaiger, K. L.; Stokes, K. K.; McCullough, R. D. A Simple Method to Generate Side-Chain Derivatives of Regioregular Polythiophene via the GRIM Metathesis and Post-polymerization Functionalization. *Macromolecules* **2003**, *36*, 61.
- (24) Bijleveld, J. C.; Zoombelt, A. P.; Mathijssen, S. G. J.; Wienk, M. M.; Turbiez, M.; de Leeuw, D. M.; Janssen, R. A. J. Poly(diketopyrrolopyrrole-terthiophene) for Ambipolar Logic and Photovoltaics. *J. Am. Chem. Soc.* **2009**, *131*, 16616.
- (25) Bijleveld, J. C.; Verstrijden, R. A. M.; Wienk, M. M.; Janssen, R. A. J. Copolymers of diketopyrrolopyrrole and thienothiophene for photovoltaic cells. *J. Mater. Chem.* **2011**, *21*, 9224.
- (26) Venkatesan, S.; Adhikari, N.; Chen, J.; Ngo, E. C.; Dubey, A.; Galipeau, D. W.; Qiao, Q. Interplay of nanoscale domain purity and size on charge transport and recombination dynamics in polymer solar cells. *Nanoscale* **2014**, *6*, 1011.
- (27) Mueller, C. J.; Singh, C. R.; Fried, M.; Huettner, S.; Thelakkat, M. High Bulk Electron Mobility Diketopyrrolopyrrole Copolymers with Perfluorothiophene. *Adv. Funct. Mater.* **2015**, *25*, 2725.
- (28) Bijleveld, J. C.; Gevaerts, V. S.; Di Nuzzo, D.; Turbiez, M.; Mathijssen, S. G. J.; de Leeuw, D. M.; Wienk, M. M.; Janssen, R. A. J. Efficient Solar Cells Based on an Easily Accessible Diketopyrrolopyrrole Polymer. *Adv. Mater.* **2010**, *22*, E242.
- (29) Li, W.; Hendriks, K. H.; Furlan, A.; Roelofs, W. S.; Meskers, S. C.; Wienk, M. M.; Janssen, R. A. Effect of the fibrillar microstructure on the efficiency of high molecular weight diketopyrrolopyrrole-based polymer solar cells. *Adv. Mater.* **2014**, *26*, 1565.
- (30) Blouin, N.; Michaud, A.; Leclerc, M. A Low-Bandgap Poly(2,7-Carbazole) Derivative for Use in High-Performance Solar Cells. *Adv. Mater.* **2007**, *19*, 2295.
- (31) Gräf, K.; Rahim, M. A.; Das, S.; Thelakkat, M. Complementary co-sensitization of an aggregating squaraine dye in solid-state dye-sensitized solar cells. *Dyes Pigm.* **2013**, *99*, 1101.
- (32) Kirby, N. M.; Mudie, S. T.; Hawley, A. M.; Cookson, D. J.; Mertens, H. D. T.; Cowieson, N.; Samardzic-Boban, V. A low-background-intensity focusing small-angle X-ray scattering undulator beamline. *J. Appl. Crystallogr.* **2013**, *46*, 1670.
- (33) Ilavsky, J. Nika: software for two-dimensional data reduction. *J. Appl. Crystallogr.* **2012**, *45*, 324.